Evaluating Realistic Performance Gains of Massive Multi-User MIMO System in Urban City Deployments

Siming Zhang, Angela Doufexi and Andrew Nix

Communication Systems & Networks Group, University of Bristol, United Kingdom
{sz1659; A.Doufexi; andy.nix}@bristol.ac.uk

***Abstract*— Massive Multiple Input Multiple Output (MIMO) is one of the key technologies in 5G, and it is envisioned to have superior spectral and energy efficiencies. This paper is the first to evaluate Massive MIMO in realistic performance metrics in heterogeneous urban environments, i.e. 20 Macrocells and 20 Picocells, providing cellular services in the city of Bristol (UK). We base our study on a 3D ray-tracing propagation channel model that uses real city maps. We also convolve our channel model with individual 3D complex polarimetric antenna radiation patterns for both base station (BS) and User Equipment (UE). We consider a system configuration with 128 elements at the BS and up to 16 receive terminals (i.e. 16 single-antenna UEs or 8 dual-antenna UEs). Eigen-beamforming precoding and a Received Bit-level mutual Information Rate (RBIR) based abstraction simulator are used on a system level. Millions of cellular links were simulated to ensure statistically relevant results. We quantify the realistically achievable capacity in terms of cell size, number of user terminals, and rank of the users, as well as the gain over traditional 4G Long-Term Evolution (LTE) networks. Overall, 128Tx-16Rx Massive MIMO (with rank-2 UEs) was found to provide up to 434% and 478% more capacity over traditional LTE Single-User MIMO with 8Tx-8Rx configuration in Macrocells and Picocells respectively.**

Keywords—Massive MU-MIMO, 3D ray-traced channel model, single- and dual-antenna UEs

I. INTRODUCTION

Mobile networks are seeing an exponential growth in data usage that is predicted to continue. In fact, [1] reported that mobile data traffic grew around 55 percent year-on-year from 2010 to 2015. Fifth Generation (5G) telecommunication standards are expected to revolutionise cellular systems and ensure significant capacity gains compared with the current 4G networks. Multiple Input Multiple Output (MIMO) technology is becoming mature. Generally, the more antennas the transmitter/receiver is equipped with, the more the possible data streams and the better the throughput performance. However, the exact level of improvement is dependent on antenna configurations and the 3-Dimensional channel multipath structure. Massive MIMO is one of the two key candidates for future 5G technologies at the physical layer (PHY), the other one being Millimeter Wave (mmWave).

In this paper, we will focus on Massive MIMO deployed at sub 6GHz bands (i.e. 2.6GHz) for cellular communications. Massive MIMO is in the realm of Multi-User (MU) MIMO and deploying hundreds of antennas or Radio Frequency (RF) chains at the base station (BS) and serving tens of User Equipments (UEs) simultaneously. The spectral and energy efficiency benefits of Massive MIMO are discussed and presented in [2] and [3]. Firstly, the large antenna array gain is believed to boost the received signal power drastically thus provide enhanced data rates and cell coverage. Secondly, the powerful beamforming and extra degrees of freedom from having more antennas at the transmitter allow not only improved MU multiplexing gain but also diversity gain. This is because the transmission and reception of signal energy can be focused into ever-smaller regions of space. Whereas in traditional LTE systems, multiplexing and diversity gains are usually trade-offs. Thirdly, the hope for better energy efficiency lies in the use of inexpensive low-power RF elements, which brings the deployment cost down. Lastly through clever UE-specific beamforming, intra- and inter-cell interference can be mitigated, further booting the system capacity. It is important to note though the signal processing power required for channel estimation, precoding and detection in real time is not trivial and needs to be considered carefully into the energy cost equation. This is an interesting research area and is currently being investigated through a testbed described in [4].

According to literature, the anticipated throughput depends on the propagation environment providing asymptotically orthogonal channels to the users. Many papers claiming superior performance gain of Massive MIMO are based on theoretical independent and identically distributed (i.i.d.) Rayleigh channels, or derived under the assumption of unlimited number of BS antennas, which are too optimistic [5]. In this paper, we investigate a Massive MIMO system with 128 BS antenna elements, and its performance in realistic urban Macrocells and Picocells. In the current literature, there has not been any study where the level of improvement can be quantified in a citywide real-world network against standard LTE networks. From the study presented in [6] and [7], the large receive power imbalance between users in realistic networks results in ill-conditioned channel matrix, together with inter-user interference, limit MU-MIMO performance. Signal to Interference and Noise Ratio (SINR) values at the UEs are often too low to support higher spatial streams. Nevertheless, it is interesting to see how much this problem can be alleviated with the large array gain of 128 BS antennas.

The major contributions of this paper are summarised below:

- Our results make use of measured 3D antenna patterns (which are omitted from the 3rd Generation Partnership Project (3GPP) channel model) combined with a realistic city-scale 3D ray-tracing channel model. Our study looks at typical Macrocell and Picocell deployments.
- Measurement campaigns like in [8] can be time and resource consuming. It is a major limitation on quantifying Massive MIMO performance and it lacks statistical relevance. With our methodology and the fact that the number of different link-level simulations in this study accumulates to 70 million, our results are statistically more accurate. To the best of the authors' knowledge, no other work has been reported at this scale.
- We focus on evaluations on a system that is equipped with 128-element antenna array at BS and up to 16 receiving chains, where the UEs can be Rank-1 or Rank-2 (i.e.16 single-antenna UEs or 8 dual-antenna UEs). Link adaptation is performed on a per-data-stream basis to optimise the expected cell capacity.
- We quantify capacity improvements as a function of the propagation environment, the number of BS and UE antennas and MIMO schemes.
- Comparisons were made to standard SU and MU-MIMO LTE performance in terms of average and cell-edge user rates and number of supported streams.

The remainder of the paper is organised as follows: Section II presents the measured BS and UE antenna element characteristics and array configurations. Section III explains our 3D channel propagation modelling process and introduces our DL network simulator with Eigen-beamforming (EBF) precoding and the Received Bit-level mutual Information Rate (RBIR) abstraction technique. Simulation results in the form of expected cell spectral efficiency (SE), cell-edge user rates and statistics for the number of supported spatial streams are given in Section IV. Finally, Section V summarises the comparison of SU, MU and Massive MIMO for realistic heterogeneous LTE-like deployments.

The following notations will be used across this paper. Normal letters represent scalar quantities and bold uppercase letters denotes matrices. $|.|$ and $(.)^H$ are absolute value, transpose, and Hermitian operators respectively. $\| \|_F$ represents the Frobenius-norm of a matrix.

II. Antenna Characterisitcs and Configurations

A. Measured BS and UE Antenna Element Patterns

As can be seen in Fig. 1(a) (left column), each Macro BS antenna element comprises of a directional patch antenna constructed on an RT/Duroid 5880 substrate. The measured far-field antenna patterns of two orthogonally polarised patch antennas are shown in Fig. 1(a) (right column). V and H refer to the vertical and horizontal polarisation components of the radiation pattern respectively and are depicted with orange (V) and blue (H) colouring. The azimuth and elevation 3dB beamwidths of the Macro BS (total power) patterns are 88° and 72° respectively for Ant 1, and 91° and 71° for Ant 2. Fig. 1(b) shows the Picocell BS and UE antenna elements, which

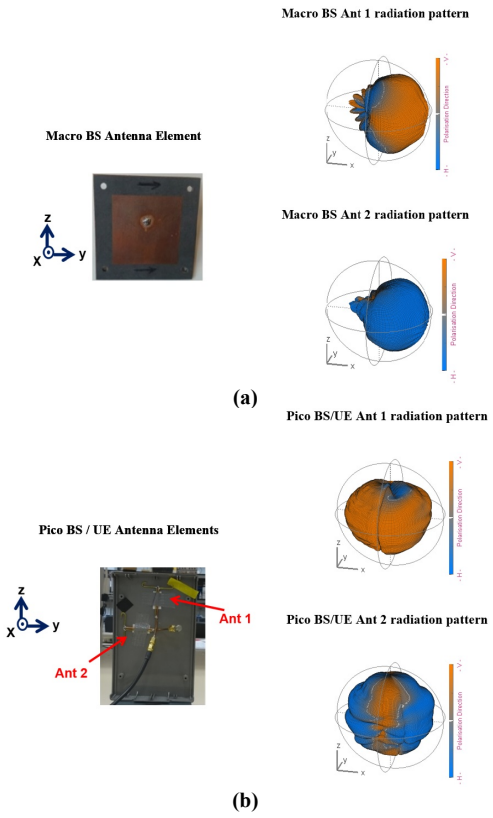

Fig. 1. Measured antenna elements and radiation patterns for Macro/ Pico BS and UE.

TABLE I. BS & UE ANTENNA ELEMENT STATISTICS

	Percentage Power in each polarisation		Max. Directivity in each polarisation (dBi)	
	Vertical	*Horizontal*	*Vertical*	*Horizontal*
MacroBS Ant 1	83%	17%	8.00	-0.49
MacroBS Ant 2	5%	95%	-5.96	8.02
PicoBS/UE Ant 1	90%	10%	5.42	-3.77
PicoBS/UE Ant 2	33%	67%	3.93	5.35

consist of a vertical (z-directed) and a horizontal (y-directed) dipole. Table I lists the percentages of radiated power in both the vertical and horizontal polarisations, along with the maximum directivity for each polarisation.

B. BS Array and UE Antenna Configurations

In the case of co-located Massive MIMO antenna arrays (Fig.2), the macro BS is a planer array with 2 rows of Uniform Linear Arrays (ULA), each comprises of 32 cross-polarised patches, hence totally 128 logical antenna elements. Half-wavelength inter-element spacing is assumed vertically and horizontally; the Pico BS is a double-stacked Uniform Circular Array (UCA) configuration with dipoles, and there is a two-wavelength separation between the stacks and half-wavelength spacing between elements on each circle. The BS array was down-tilted by 10° in our virtual network simulations to optimise the in-cell signal to noise ratio (SNR). For Macrocells, the largest dimension of our array is 1.85m (16 wavelengths), for Picocells, the diameter of our circular array is 0.59m. If we approximate the antenna array as one single radiating entity, for antennas physically larger than a half-wavelength of the radiation they emit, Fraunhofer

distance provides the limit between the near and far field. The Fraunhofer distance is $d_f = \frac{2D^2}{\lambda}$, where D is the largest dimension of the antenna, i.e. the physical length of an antenna, or the diameter of a "dish" antenna, and λ is the wavelength of the radio wave. Having an antenna electromagnetically longer than one-half the dominated wavelength emitted considerably extends the near-field effects, especially that of directional antennas. In our case, $d_{f\_Macro} = 59m$ and $d_{f\_Pico} = 6m$. In our ray-tracing database, we have almost all the users situated within the far field of the antenna array. Furthermore, recent literatures have considered the angular power spectrum (APS) and cluster power variations over physically large arrays, for instance the measurement campaign in [8]. The 128-element ULA and UCA were found to have different APS footprints across the arrays through a limited number of measurement points. However, this effect is beyond the scope of this work, so large-scale fading across the BS arrays are not modelled. To take this into consideration in our ray-tracing channel model in the future, the point expansion technique can be replaced after statistically analysing the visibility of power clusters across the antenna array from measurements.

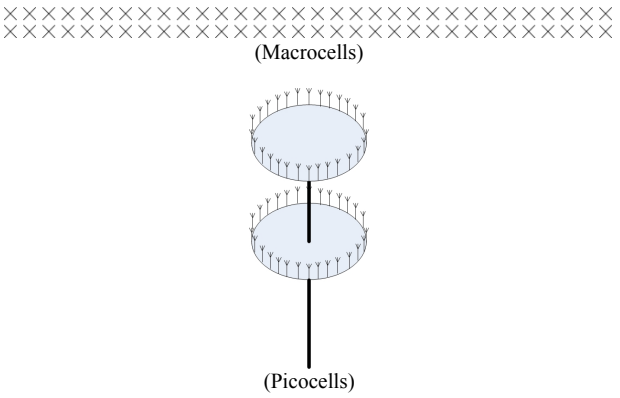

Fig. 2. BS antenna array configuration for macrocells and picocells

III. Channel Model And Sysytem Model

A. Ray-Tracing and Parameters

The channel propagation study was performed using an outdoor 3D ray-tracer [9]. The tool was used to generate the channel sets behind many of the statistics now specified in the 3D extension of the 3GPP channel model [10], [11], [12]. A 17.6km^2 laser-scanned database of Bristol (UK) was used, which comprises buildings, foliage and terrain layers. Table II shows a summary of the ray-tracing parameters used. Note that antennas were assumed to be isotropic at both ends of the link in the ray model in order to generate a *pure* channel. In post processing any type of transmit and receive antenna pattern and array geometry can be applied as a spatial, polarisation and phase convolution process. Point-source ray tracing was performed from the BS to each UE. As an example, Fig.3 depicts the traced paths in a MU-MIMO scenario for a Picocell (bottom left corner) and a triple-sectorised Macrocell (center) in the centre of Bristol City. The underlying colour of the rays indicates the received power, and the brighter the colour the higher the power. The ray model provides information not only on the amplitude, but also the phase, time delay, angle-of-departure (AoD) and angle-of-arrival (AoA) of each multi-

TABLE II. Summary of Ray-Tracing Parameters

	Macro cells	Pico cells
Environment	17.6km^2 area of central Bristol (UK)	
Frequency	2.6 GHz	
BS mounting	On rooftops of buildings at a height of 3m above rooftop level	On lamp-posts at a height of 5m above ground level
Number of BSs and UEs	20 three-sector cells 300 random UEs/sector (Total 900 UEs/cell)	20 cells 150 random UEs per cell
User locations	50-1000 m from BS 1.5m above ground level	5-150 m from BS 1.5m above ground level
BS power to antenna port	44 dBm	30 dBm
BS height	Ranging from 7m to 50m	5 m above ground level
Antennas	Isotropic at both ends of the link	
Minimum receiver sensitivity	-120 dBm (only links with two or more traced rays were considered)	
Link direction	Downlink (From BS to UE)	

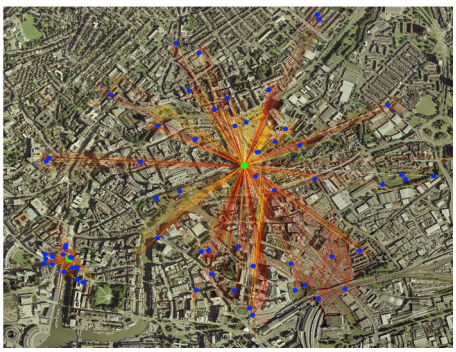

Fig. 3. Modelling of MPCs for 3D MU-MIMO in a sectorised Macrocell and Picocell (*green dots: BS locations, blue dots: UE locations*)

-path component (MPC) linking the BS and UE. The phase of each MPC was then adjusted according to the transmitting/receiving antenna's relative distance from a zero-phase reference point on the array. The complex gain of each MPC was also adjusted according to the transmitting/receiving antenna E-field pattern response for the corresponding AoD/AoA and polarization. This gives EIRP values of approximately 52dBm and 36dBm for Macrocells and Picocells respectively.

B. Network Simulator and Parameters

An LTE-like downlink simulator was developed to quantify the average and cell-edge data throughput performance. Table III lists the key parameters of this simulator. The full Channel State Information (CSI) was assumed to be available at the BS and UEs. Therefore, the closed-loop channel precoding method, Eigen-Beamforming (EBF), can be evaluated. Consequently, our results represent an upper-bound performance of a Massive MIMO system. Other linear precoding methods, such as zero-forcing beamforming, will be evaluated and compared in future work. Since our BS antenna array configuration is fixed, we keep the transmit power to antenna port constant at the BS as the number of receiving chains *K* increases.

TABLE III. SUMMARY OF SIMULATION PARAMETERS

Parameter	Assumption
Transmission bandwidth	20 MHz
FFT size	2048
Number of occupied subcarrier	1200
Number of OFDM symbols per time slot	7
Channel State Information	Perfect
Channel coding	Turbo
Noise Floor	-96 dBm
PER threshold	0.1
MCS modes	QPSK1/2,QPSK3/4,16QAM1/2, 16QAM3/4,64QAM1/2,64QAM3/4
MIMO precoding	8x8/16x8 SU-EBF and MU-EBF 128x8 and 128x16 MU-EBF
UE Configuration (SU/MU)	8-antenna UE/ Single-antenna or Dual-antenna UE
SNR range for MU-MIMO	-20 dB to 25 dB
Multi-User Grouping	100 random iteration per sector/cell
Peak Capacity	1.2Gbps

C. Multiuser MIMO with Eigen-Beamforming

It is demonstrated in numerous studies, such as [8] and references therein, that linear precoding can achieve nearly optimal performance capacity-wise when the number of UEs is also large and the environment is rich with scattering. In this paper, Eigen-beamforming is performed at baseband and requires the channel to be known perfectly both at the BS and the UEs. In the following simulations we investigate 8-layer beamforming with 8-antenna single UE or multiple Rank-1 or Rank-2 UEs respectively. In MU-MIMO cases, co-scheduled UEs needs to be all Rank-1 or all Rank-2. In Rank-2 UE scenarios, BS will determine whether single-layer or dual-layer beamforming should be used for each user in the group so that the sum capacity can be maximised.

We firstly normalise the overall users' channels so that the channel coefficients has unit average energy over all M antenna ports, N users and across all L subcarriers. This is achieved through:

$$\mathbf{H}_{norm,l,t} = \sqrt{\frac{\mathrm{M*N*L}}{\sum_{\mathrm{l=1}}^{\mathrm{L}} \|\boldsymbol{H}_l^{raw}\|_F^{\,2}}}\,\boldsymbol{H}_l^{raw} \qquad (1)$$

where $\boldsymbol{H}_{norm,l,t}$ denotes the normalized channel matrix at l^{th} subcarrier and at time instance t. Thereby, we keep the difference in channel attenuation between users, as well as variations over antenna elements and frequencies. We then perform singular value decomposition (SVD) of the overall frequency domain channel matrix, $\boldsymbol{H}_{norm,l,t}$, and performing Eigen-Beamforming.

$$\boldsymbol{H}_{norm,l,t} = \boldsymbol{U}_{l,t}\boldsymbol{S}_{l,t}{\boldsymbol{V}_{l,t}}^{H} \qquad (2)$$

at l^{th} subcarrier and at time instance t, $\boldsymbol{U}_{l,t}$ and $\boldsymbol{V}_{l,t}$ represent the left and right unitary matrices, and $\boldsymbol{S}_{l,t}$ is a diagonal matrix with singular values being the diagonal elements and arranged in decreasing order. Since each stream is pair-wise orthogonal, hence zero inter-stream-interference, the effective SINR of the i^{th} stream is its SNR and can be calculated as below,

$$SINR_i = P_{tx,i} * \frac{|\lambda_i|^2}{|\sigma_0|^2} \qquad (3)$$

where λ_i represents the i^{th} singular value, and σ_0 is the standard deviation of the noise. $P_{tx,i}$ is the transmit power for the i^{th} data stream. Here we assume the transmit power is equally allocated between streams, while maintaining a normalised total power constraint of unity. With increasing the number of transmit antennas, the array gain increases and we choose to harvest this as improved interference cancellation, i.e. better user orthogonality instead of increased receive SNR at the users. In other word, this essentially keeps the Effective Isotropic Radiated Power (EIRP) constant as the BS antenna number grows. This is usually for complying with the regulatory requirements, as well as to make fair and realistic comparisons of different settings. Through investigating the Eigen-structure of the channel, we can accurately and efficiently estimate the system-level capacity prediction with the RBIR abstraction engine.

D. RBIR Abstraction Simulator

To perform system level analysis in a computationally efficient and scalable manner, a PHY layer abstraction technique RBIR was used to predict the average packet error rate (PER) for a UE from its effective SINR for a given channel realisation across the allocated OFDM subcarriers. This technique was fully described in [13] and [14]. Without sacrificing accuracy, abstraction is many hundreds of times faster than full bit-level simulation, which is essential to Massive MIMO evaluations.

Optimal modulation and coding scheme (MCS) selection was performed per UE based on the mode that achieved the highest link throughput on the condition that the PER does not exceed 10%. The expected throughput was then calculated using the peak error-free data rate (for the supported number of spatial streams and MCS) and the PER, and averaged over 1000 channel realisations. Although theoretic receive powers can be very high, in practice Error Vector Magnitude (EVM) specifications limit the maximum SNR observed at the UE. For this study we assumed a peak SNR of 25dB at the UE (which translates to an EVM of around 6%). Furthermore, any UE with an SNR below -20dB was excluded from MU-MIMO analysis.

IV. DOWNLINK PERFORMANCE IN MASSIVE MIMO

Due to convergence difficulties in SVD operations from badly scaled channel matrixes, which is the result of large variances of receive power between co-scheduled UEs, the system configuration was limited to up to 128Tx-16Rx (for simplicity 128x16 will be used for the rest of the paper). At least 100 iterations will be run per sector/cell to ensure statistically relevant results. Comparisons are provided from SU- and MU-MIMO to Massive MIMO in terms of the likelihood of supporting multiple data streams, the overall cell spectral efficiencies and other Quality of Service (QoS) parameters. SE is in unit of bits per second per Hertz (bps/Hz) per Sector for Macrocells and per cell for Picocells.

A. What are the capacity benefits of Massive MIMO?

Fig.4 shows the average SE in 128x8 and 128x16 configurations with dual-antenna UEs in comparison with SU and MU cases. With the best Massive MIMO configuration, it provides up to 434% and 478% capacity gain compared to SU-8x8 in Macrocells and Picocells respectively. The percentages reduced to 309% (Macrocells) and 261% (Picocells) when

comparing to MU-MIMO 8x8. It is believed that the improvement mainly comes from the antenna array gain of 128 elements, as well as more receiving terminals. The expected SE can only reach half of the full capacity of the system. It is important to note that random user grouping is assumed in this study, therefore there is a high probability that cell-centre users could be co-scheduled with cell-edge users, which leads to ill-conditioned MU channel matrix and less desirable average cell capacity. In actuality, the gain will be less than the prediction presented in [2-5].

Cell-edge user rate is often interpreted as the 5%-tile user rate. Table IV lists the 5%-tile SE for the various scenarios under consideration (MU/ Massive MIMO cases are with rank-1 UEs). MU 8×8 and 16×8 schemes demonstrate good performance, quadrupling and doubling SE over SU counterparts respectively. The claim stands true for both Macro and Picocells. This implies a significant QoS enhancement. As for Massive MIMO, performance improved drastically with 128x16 configuration offering more than 15 times and 18 times efficiency than SU 8x8.

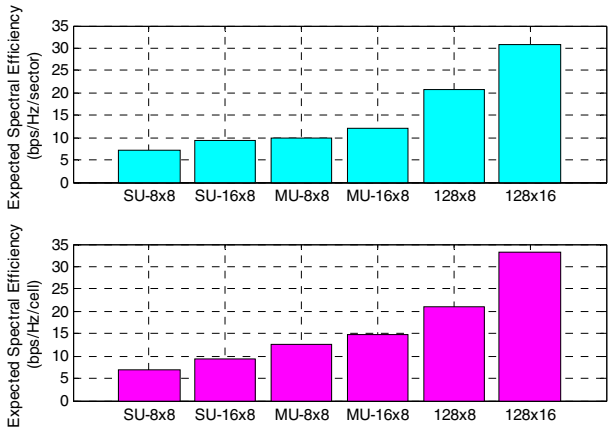

Fig. 4. Expected Spectral Efficiency of SU, MU and Massive MIMO in Macrocells(upper) and Picocells(bottom)

TABLE IV. 5 PERCENTILE SE IN SU, MU AND MASSIVE MIMO

5% SE (bps/Hz/cell)	SU 8x8	SU 16x8	MU 8x8	MU 16x8	128x8	128x16
Macrocells	0.78	1.57	3.78	3.78	8.37	12.15
Picocells	0.79	1.64	3.78	3.78	7.95	14.41

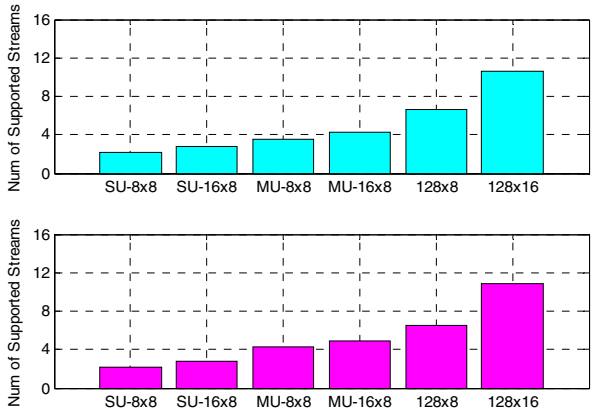

Fig. 5. Average number of maximum supported streams of SU, MU and Massive MIMO in Macrocells(upper) and Picocells(bottom)

It is worth noting that an exhaustive search of all MCS modes and supported numbers of spatial streams was performed for co-scheduled users at each simulation iteration, enabling rapid switching to and from higher spatial stream numbers on a channel snapshot-by-snapshot basis. In a practical system, such gains in data rate will be less impressive since the link speed selection algorithm is unlikely to switch so rapidly in time.

B. How many spatial streams are supported in practice?

Fig.5 shows the comparison on maximum supported number of data streams averaged across 20 Macrocells and 20 Picocells with dual antenna users. On average, 128x8 can support more than 6 data stream and 128x16 can support more than 10 data streams in Macrocells and Picocells, compared with less than 3 streams in SU case with 8 receive antennas. These stream numbers are well below the full rank, which is expected after seeing the capacity performance in Fig.4. Since the supported number of streams is greater than the number of users in both configurations, it is safe to say dual-stream operation is definitely present in the system. When comparing MU-16x8 and Massive-128x8, there is only 56% more capacity achieved. Considering the 100 more antennas and the expensive RF chains behind each antenna, this gain is not impressive enough to justify the deployment cost. However, it is worth pointing out that scaling the receiver end, i.e. multiplexing more users and equipping UE with more antennas, is encouraging. Although the capacity is not doubled, we can see at least 4 more data streams are supported when increasing RX from 8 to 16. Interestingly, by having excessive antennas at the BS, Picocells no longer provide much advantage against Macrocells as used to be in the SU and MU-MIMO cases. The large antenna array gain and the dimension of the actual array bridge the gap between cell types in terms of receive SNRs and angular spreads in both the azimuth and elevation domains.

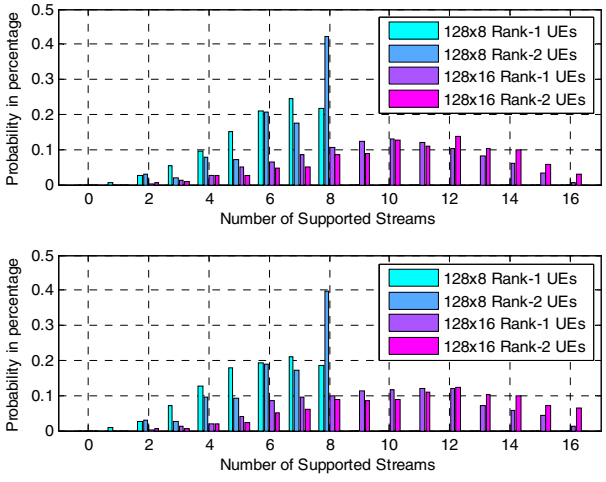

Fig. 6. Histogram of average supported number of spatial streams in Macrocells (upper) and Picocells(bottom)

Fig.6 shows the histogram of supported streams in Massive MIMO across all cells. It is worth noting that the number of streams here is the maximum that can be supported in the

current channel conditions, not necessarily the optimal operational mode. Therefore, this histogram graph should not be treated as a translation of the spectral efficiency performance, but an indicator of the channel's Eigen-structure. For the dual-antenna UEs, the most used streams in 128x8 case is surprisingly full-rank 8 streams, while about 12 streams are mostly supported in 128x16. When single-antenna UEs are concerned, one stream less is generally expected. This leads us to believe there is certain truth behind a common understanding in Massive MIMO literature that the ratio between the BS and UE antennas needs to be no less than 10 to support full rank in realistic scenarios.

C. How does the number of user antennas affect capacity?

TABLE V. CAPACITY PERFORMANCE OF RANK-1 & RANK-2 UES

Avg. SE (bps/Hz/cell)	Macrocells Rank-1	Macrocells Rank-2	Picocells Rank-1	Picocells Rank-2
MU-8x8	7.9	10.0 (26.2%)	10.0	12.7 (27.2%)
MU-16x8	9.3	12.1 (29.6%)	12.0	14.7 (23.1%)
128x8	18.0	20.7 (15%)	18.1	21.1 (16.3%)
128x16	27. 1	30.8 (13.7%)	29.0	33.2 (14.5%)

Table V focuses on comparison between Rank-1 and Rank-2 UEs in terms of feasible spectral efficiency and relative improvement percentages in MU and Massive MIMO cases. Dual antenna UEs achieve on average 25% more capacity than single antennas UEs in MU-MIMO, and 15% when it comes to Massive MIMO. Similar to the possible reasons explained for MU-MIMO, the benefit of diversity gain from dual-antenna UEs is diminishing when the BS array grows large.

V. CONCLUSIONS

This paper has quantified the theoretic system level benefits of Massive MIMO in heterogeneous LTE-like urban environments using classic Eigen-Beamforming precoding method. Tens of millions of ray-traced cellular links in 20 Macrocells and 20 Picocells were evaluated to ensure statistical relevance. Performance metrics include average cell SE, cell-edge SE and the number of supported data streams.

Overall, through our investigation in realistic channels, with random UE grouping, the best Massive MIMO configuration, i.e. 128x16 with rank-2 UEs, provided up to 434% (Macrocells) and 478% (Picocells) more capacity over SU-MIMO-8x8, and 309% (Macrocells) and 261% (Picocells) over MU-MIMO-8x8 respectively. Dual-antenna UEs gained approximately 15% more capacity than single-antennas UEs in Massive MIMO. Finally, the benefit of diversity gains from the UEs having more antennas falls away as the dimensions of the BS array increases.

ACKNOWLEDGMENT

The authors would like to acknowledge the technical and financial support of Timothy Thomas and Amitava Ghosh at Nokia Networks (Chicago, USA).

REFERENCES

[1] Ericsson Mobility Report, Accessed at: http://www.ericsson.com/mobility-report, Aug 2015

[2] F. Rusek, D. Persson, B. Lau, E. Larsson, T. Marzetta, O. Edfors, F. Tufvesson, "*Scaling up MIMO: Opportunities and Challenges with Very Large Arrays,*" IEEE Signal Processing Magzine, Jan 2013.

[3] J. Hoydis, S. Brink, M. Debbah, "*Massive MIMO in the UL/DL of Cellular Networks: How Many Antennas Do We Need?*", IEEE Journal on Selected Areas in Communications, Feb 2013.

[4] P.Harris, S.Zhang , A.Nix, M.Beach, S.Armour, A.Doufexi, "*A Distributed Massive MIMO Testbed to assess Real-World Performance & Feasibility*," in Proceedings of IEEE VTC-Spring 2015

[5] T. L. Marzetta, "Noncooperative cellular wireless with unlimited numbers of base station antennas", IEEE Trans. Wireless Commun., vol. 9,no. 11, pp.3590 -3600, 2010

[6] S. Zhang, D. Kong, E. Mellios, A. Doufexi and A. Nix, "*Comparing Theoretic Single-User and Multi-User Full-Dimension MIMO Data Throughputs in Realistic City-Wide LTE-A Deployments,*" in Proceedings of IEEE Globecom 2015.

[7] S.Zhang, D. Kong, E. Mellios, G. Hilton, A. Nix, T. Thomas, A. Ghosh, "*Impact of BS Antenna Number and Array Geometry on Single-User LTE-A Data Throughputs in Realistic Macro and Pico Cellular Environments,*" in Proceedings of IEEE WCNC 2015

[8] X. Gao, O. Edfors, F. Rusek, and F. Tufvesson, "*Massive MIMO Performance Evaluation Based on Measured Propagation Data,*" IEEE Transactions on Wireless Communications, VOL. 14, NO. 7, Jul 2015

[9] K.H. Ng, E.K. Tameh, A. Doufexi, M. Hunukumbure, and A.R. Nix, "*Efficient Multi-element Ray Tracing With Site-Specific Comparisons Using Measured MIMO Channel Data,*" IEEE Transactions on Vehicular Technology, vol. 56, issue 3, pp. 1019-1032, May 2007.

[10] T. Thomas, F. W. Vook, E. Visotsky et al., "*3D extension of the 3GPP/ITU channel model,*" in Proceedings of IEEE VTC-Spring, May 2013.

[11] Text Proposal R1-130497, "*3D Channel Modeling Issues and 3D Channel Model Proposal, 3GPP TSG-RANWG1*".

[12] Text Proposal R1-130500, "*Detailed 3D Channel Model, 3GPP TSG-RANWG1*".

[13] D. Halls, A. Nix, and M. Beach, "*System level evaluation of UL and DL interference in OFDMA mobile broadband networks,*" in Proceedings of the IEEE WCNC, March 2011

[14] Y.Q Bian, A.R. Nix, E.K Tameh and J.P McGeehan, '*MIMO–OFDM WLAN Architectures, Area Coverage, and Link Adaptation for Urban Hotspots*,' IEEE Transactions on Veh. Tech, vol.57, no.4, July 2008.